Investigating the Antimalarial Action of 1,2,4-Trioxolanes with Fluorescent Chemical Probes

ARTICLE *in* JOURNAL OF MEDICINAL CHEMISTRY · DECEMBER 2011

Impact Factor: 5.45 · DOI: 10.1021/jm2012003 · Source: PubMed

6 AUTHORS, INCLUDING:

Adam Renslo
University of California, San Francisco
87 PUBLICATIONS **1,569** CITATIONS

SEE PROFILE

Published in final edited form as:
J Med Chem. 2011 December 8; 54(23): 8207–8213. doi:10.1021/jm2012003.

Investigating the Antimalarial Action of 1,2,4-Trioxolanes with Fluorescent Chemical Probes

Carmony L. Hartwig[†,‡,◇], **Erica M.W. Lauterwasser**[§,◇], **Sumit S. Mahajan**[§], **Jonathan M. Hoke**[†], **Roland A. Cooper**[†,¶,*], and **Adam R. Renslo**[§,*]

[†]Department of Biological Sciences, Old Dominion University, Norfolk, VA

[‡]Malaria Research and Reference Reagent Resource Center (MR4), American Type Culture Collection, Manassas, VA

[§]The Small Molecule Discovery Center and Department of Pharmaceutical Chemistry, University of California, San Francisco, CA

[¶]Department of Natural Sciences and Mathematics, Dominican University of California, San Rafael, CA

Abstract

The 1,2,4-trioxolanes are a new class of synthetic peroxidic antimalarials currently in human clinical trials. The well known reactivity of the 1,2,4-trioxolane ring towards inorganic ferrous iron and ferrous iron heme is proposed to play a role in the antimalarial action of this class of compounds. We have designed structurally relevant fluorescent chemical probes to study the sub-cellular localization of 1,2,4-trioxolanes in cultured *Plasmodium falciparum* parasites. Microscopy experiments revealed that a probe fluorescently labeled on the adamantane ring accumulated specifically in digestive vacuole-associated neutral lipid bodies within the parasite while an isosteric, but non-peroxidic congener did not. Probes fluorescently labeled on the cyclohexane ring showed no distinct localization pattern. In their sub-cellular localization and peroxidative effects, 1,2,4-trioxolane probes behave much like artemisinin-based probes studied previously. Our results are consistent with a role for adamantane-derived carbon-centered radicals in the antimalarial action of 1,2,4-trioxolanes, as hypothesized previously on the basis of chemical reactivity studies.

Keywords

Antimalarials; 1,2,4-Trioxolanes; Free radicals; Heme; Lipid Peroxidation

Introduction

The World Health Organization has recommended artemisinin combination therapy (ACT[a]) as the preferred first-line treatment for uncomplicated *Plasmodium falciparum* malaria.[1] Artemisinin and its semi-synthetic analogs are derived ultimately from the plant source,

[*]To whom correspondence should be addressed. RAC: Phone: (415) 482-1887. Fax: (415) 482-1972. roland.cooper@dominican.edu. ARR: Phone: (415) 514-9698; fax: (415) 514-4507; adam.renslo@ucsf.edu.
[◇]These authors contributed equally to this work.

Supporting Information Available: Copies of ^{1}H NMR spectra for analogs **5-8**. This material is available free of charge via the internet at http://pubs.acs.org.

[a]Abbreviations Used: ACT, artemisinin combination therapy; DFO, desferrioxamine; PfATP6, *Plasmodium falciparum* sarco/endoplasmic reticulum Ca^{2+} ATP-ase; SERCA, sarco/endoplasmic reticulum Ca^{2+} ATP-ase; DV, digestive vacuole; TEMPO, (2,2,6,6,-tetramethylpiperidin-1-yl)oxyl; NLB, neutral lipid bodies; dDHA, deoxydihydroartemisinin.

Artemisia annua. The need for affordable and reliably available antimalarial therapies has spurred research into alternate methods for their manufacture[2] and also the search for wholly synthetic molecules that confer an analogous antimalarial activity. An important advance with regard to the latter has been the appearance of various synthetic peroxides,[3] most notably the investigational agent arterolane (OZ277)[4] which contains a sterically hindered 1,2,4-trioxolane ring (Chart 1). Arterolane is currently in Phase III clinical trials in combination with piperaquine whereas a next-generation trioxolane (OZ439) with improved in vivo properties is in early-stage clinical trials.[5]

The antimalarial action of the artemisinins, 1,2,4-trioxolanes, and other synthetic peroxides is clearly associated with the presence of a peroxide bond, though the precise molecular mechanism of activity remains a topic of active research and healthy debate. Largely undisputed in the field is the importance of ferrous iron (putatively inorganic Fe^{II}, free heme, or ferrous hemoglobin heme) in the activity of antimalarial peroxides, and the likely involvement of primary and/or secondary carbon-centered radical metabolites.[3, 6, 7] For example, isosteric but non-peroxidic analogs of artemisinin and arterolane are generally at least 1000-fold less potent against *P. falciparum* parasites[8, 9] and the non-peroxidic isosteres do not antagonize the activity of their peroxidic congeners.[10] Also favoring an iron-dependent activation hypothesis are findings that artemisinin and arterolane are potently active primarily against hemoglobin digesting parasites[8] while iron chelating reagents like desferrioxamine (DFO) antagonize their action against *P. falciparum*.[9, 11]

The *P. falciparum* sarco/endoplasmic reticulum Ca^{2+} ATP-ase (PfATP6/SERCA) has been proposed as a specific target of the artemisinins.[9] However, recent studies have questioned this hypothesis. The Ca^{2+}-ATPase activity of purified PfATP6 was insensitive to inhibition by artemisinin and derivatives, but sensitive to known SERCA inhibitors[12]. Morphological studies in *P. falciparum* have shown that initial cellular damage by artemisinin and experimental trioxanes is directed towards the digestive vacuole (DV) as opposed to the endoplasmic reticulum at relevant drug concentrations.[13] Arterolane binds PfATP6 about 5000-fold more weakly (K_i = 7900 nM) than its antimalarial potency, making this an unlikely target of trioxolanes.[11]

Other investigators have advanced a role for heme-artemisinin and heme-trioxolane conjugates in the antimalarial action of these agents. Supporting this view are findings that artemisinins alkylate human ferrous hemoglobin in vitro[14] and that heme-artemisinin conjugates could be isolated from artemisinin-treated mice infected with *P. vinckei*, but not from uninfected mice given an equivalent dose of drug.[15] Attempts to correlate antimalarial activity with in vitro reactivity towards heme have been complicated by the fact that artemisinins are generally less efficient than trioxolanes at alkylating heme in vitro,[16, 17] and are similarly poor at intercepting radical spin traps such as (2,2,6,6,-tetramethylpiperidin-1-yl)oxyl (TEMPO).[10, 17] Thus it is problematic to interpret such correlation data across structural classes of peroxides. However, within a congeneric series of 1,2,4-trioxolane analogs antimalarial activity was indeed well correlated with the extent of heme alkylation in vitro.[16] Finally, a recent finding[18] that artemisinin action requires the presence of hemoglobin degradation products is also consistent with a role for heme in the mode of action of artemisinins.

Heme conjugates have been proposed to confer parasite toxicity by interference with hemozoin formation[19] or by disruption of DV morphology.[13] One of us (Cooper) recently demonstrated with fluorescently-labeled probes the peroxide-dependent localization of artemisinin species (or their reaction products) within DV-associated neutral lipid bodies (NLB).[20] This localization was correlated with oxidative damage to cellular lipids as determined *in situ* using an oxidation sensitive BODIPY lipid probe and also via analysis of

lipids extracted from treated parasites. Recent experimental work suggests that neutral lipids can serve as a catalyst for hemozoin formation within the DV[21] and that 1,2,4-trioxolanes (and also tetraoxanes) mediate phospholipid peroxidation in vitro upon exposure to ferrous iron sources.[22] Hence, current evidence indicates that both free ferrous heme and neutral lipids are present in the DV, producing a chemical environment favorable for the homolytic cleavage of peroxide bonds. We now describe the design and synthesis of a new series of fluorescent chemical probes intended to reveal the intra-cellular reactivity and sub-cellular localization of 1,2,4-trioxolane antimalarials and their reaction products.

Results and Discussion

Structurally relevant fluorescent probes were designed to explore the intra-cellular reactivity of 1,2,4-trioxolanes, and more specifically to determine if such reactivity was consistent with trioxolane fragmentation mechanisms proposed previously[7] on the basis of in vitro chemical reactivity studies. In the canonical mechanism (Scheme 1), reduction of the peroxide bond with Fe^{II} occurs regioselectively at the less hindered oxygen atom, presumably via the equatorial-peroxide conformer which best exposes the peroxide σ* antibonding orbital for reaction. An initial oxygen-centered radical quickly collapses to a secondary carbon-centered radical **2,** which reacts further to afford products of radical self-quenching (**3a** and **3b**) and cyclohexanone (**4**). When the reaction is carried out it the presence of a radical spin trap reagent such as 4-(oxo)-TEMPO, high yields of the adamantane-derived TEMPO conjugate **3c** are obtained.[7] It is the adamantane-derived radical species **2** that is proposed to confer antimalarial effects in parasites, putatively via reaction with heme[16] and/or by mediating the peroxidation of phospholipid. [20, 22]

If the chemical processes described above occur also in the parasite, one predicts that adamantane- and cyclohexane-derived reaction products should have different sub-cellular localization patterns. In recent studies employing cyclohexane-linked fluorescent probes, only diffuse labeling of the parasite cytosol or DV was observed.[11, 23] These studies did not address the possibility that such probes might well fragment within the parasite to produce fluorescently labeled cyclohexanone products without any predicted target or role in antimalarial action. To reveal the fates of both halves of 1,2,4-trioxolanes, we designed the probes **5** and **6,** in which a dansyl fluorophore is attached via the adamantane or cyclohexane ring, respectively. The non-peroxidic dioxolane probe **7** was prepared to test the peroxide-dependence of antimalarial activity and sub-cellular localization, while the non-fluorescent trioxolane **8** was used in competition experiments and in experiments with the BODIPY-lipid probe.

Compounds **5–8** were synthesized using established synthetic methods (Scheme 2).[24] No attempt was made to isolate the final compounds as single stereoisomers, a decision that was largely pragmatic but is justified in light of previous findings that stereoisomeric 1,2,4-trioxanes possess similar antimalarial activities.[25] The antimalarial activity of compounds **5–8**, artemisinin, and arterolane[4] were determined using a standard 72 hour microplate assay with SYBR Green I detection to determine the half-maximal inhibitory concentration (IC_{50}) of each compound against *P. falciparum* parasites (Table 1).[26, 27] Importantly, the fluorogenic probes **5** and **6** retain a low nanomolar effect on parasites, as does compound **8.** As expected, the non-peroxidic dioxolane probe **7** was at least 1000-fold less potent than **5** against parasites. Thus, the introduction of the dansyl group does not prevent permeability across erythrocyte and parasite membranes; compounds **5–8** appear to be valid probes for studies of trioxolane action.

Next we examined fluorescence localization of compounds **5–8** in living intra-erythrocytic *P. falciparum* parasites. Similar to previous findings[11, 23] with other cyclohexane-linked

probes, the trioxolane probe **6** demonstrated a cytoplasmic accumulation pattern within mature parasites, with no distinct sub-cellular localization (Figure 1A). In contrast, we found that application of an equimolar concentration (500 nM) of the adamantyl-linked trioxolane **5** resulted in a punctate localization within small spherical structures closely associated with the parasite DV (Figure 1B). This precise compartmentalization pattern has been demonstrated previously by our laboratory to be evidence of fluorescent trioxane metabolite accumulation within parasite NLB.[20] NLB are small droplets consisting of neutral lipids hypothesized to promote hemozoin crystallization following hemoglobin digestion and free heme release within the parasite DV.[28, 29] In contrast to our observations with trioxolane **5** we found that the isosteric but non-peroxidic dioxolane probe **7** failed to exhibit NLB localization and instead distributed broadly throughout the parasite cytosol and membranous structures (Figure 1C). As noted in previous in vitro studies, the adamantane ring is the site of carbon radical formation (Scheme 1) as well as the site of covalent reaction with heme in vitro.[16] Therefore, the specific localization to NLB observed with trioxolane **5** but not trioxolane **6,** strongly suggests that NLB accumulation is associated with adamantane-derived products, possibly including heme conjugates. Our findings that dioxolane **7** accumulation patterns did not mirror those of trioxolane **5,** indicates that localization of fluorescent metabolites within NLB is endoperoxide-dependent, and therefore almost certainly involves reaction with heme or other ferrous iron sources in the parasite. The very different localization patterns observed for analogs **5–7** also establishes that NLB accumulation of **5** is not an artifact of the dansyl moiety itself.

Specific and endoperoxide-dependent trioxolane localization within NLB was clearly demonstrated by competition experiments between non-fluorescent trioxolane **8** and trioxolane **5.** We found that pre-treatment with trioxolane **8** significantly (n=3; p=0.009) reduced the number of detectable fluorescent NLB by 66.8 ± 10.2% within mature parasites labeled by trioxolane **5** (Figure 2B). In contrast, pre-treatment with methanol vehicle had no effect on trioxolane **5** distribution as evidenced by the expected exclusive pattern of fluorescent accumulation within NLB (Figure 2A). The ability of the non-fluorescent trioxolane **8** to competitively block NLB accumulation by fluorescent trioxolane **5** supports a common mechanism of action for these two trioxolane analogs and further suggests *a specific reaction partner* (plausibly free heme) that is depleted by pre-treatment with **8** in this experiment.

Earlier research into the possible mechanism of trioxane (artemisinin) action provides evidence that artemisinin is capable of mediating the peroxidation of a parasite membrane-incorporated peroxyl-radical sensor (BODIPY 581/591 C_{11}) following a relatively short incubation period (~ 5 h), thereby suggesting that oxidation reactions initiated directly by the endoperoxide or by redox-active heme-artemisinin conjugates may ultimately lead to parasite death.[20] To examine the ability of trioxolanes to induce peroxidation reactions in the parasite, we incubated parasite cultures at each major asexual stage for 2.5 h with 250 nM of trioxolane **8,** artemisinin, or the non-peroxidic artemisinin derivative deoxydihydroartemisinin (dDHA), followed by 0.5 h incubation with the BODIPY 581/591 C_{11} (Figure 3). dDHA is roughly 100-fold less potent than typical artemisinin derivatives.[20] The BODIPY probe is a useful peroxyl radical oxidation sensor as radical cleavage of the butadienyl group results in a loss of red spectral emission.[30] We found that exposure to trioxolane **8** induced peroxidation of membrane-incorporated probe in all asexual stages (Figure 3A), similar to the artemisinin control group (Figure 3B), as evidenced by a shift from red to yellow/green fluorescence. Late-stage parasites exhibited a greater degree of peroxidation than ring stages. In contrast, the dDHA derivative failed to induce peroxidation at any asexual stage, confirming that peroxidation was endoperoxide-dependent (Figure 3C).

Conclusions

Initial studies with **5–8** suggest that these compounds are useful probes for dissecting the reactivity and localization of 1,2,4-trioxolanes in live *P. falciparum* parasites. Our initial studies provide evidence that the trioxolane ring does fragment within parasites and that fragmentation is accompanied by the accumulation in NLB of reaction products derived from the adamantane moiety. These results are thus consistent with the fragmentation mechanism proposed previously on the basis of in vitro chemical reactivity studies, and indirectly support the proposed involvement of covalent heme adducts, which may become localized in NLB due to the presence of free heme in DV lipids. Our findings further suggest a common mechanism of action for trioxolane and trioxane antimalarials involving peroxidative damage to the parasite mediated either by the endoperoxide species itself and/or by covalent adducts derived from them.

Experimental Section

In vitro cultures of *Plasmodium falciparum* parasites

P. falciparum strains FCB and 7G8 (ATCC repository; MRA-926) were cultured in either human A^+ or AB^+ erythrocytes at 37 °C using RPMI 1640 media supplemented with 0.25% $NaHCO_3$, 25 mM HEPES, 0.37 mM hypoxanthine, 0.01 mg/ml gentamicin and either 0.5% Albumax I (Invitrogen) or 10% human serum, under an atmosphere of 90% nitrogen, 5% oxygen, and 5% carbon dioxide.

Susceptibility testing

Test compounds were prepared as 10 mM stock solutions in DMSO or MeOH and stored at −30 °C. The in vitro susceptibility of *P. falciparum* to test compounds was measured in a 72 h microplate growth inhibition assay using SYBR Green I (Molecular Probes) detection as described.[26, 27] Parasites were introduced into the assay only when a majority of the parasites (typically ≥80%) where at ring stage. Mean half-maximal inhibitory concentrations (IC_{50} values) were derived by plotting percent growth inhibition against log compound concentration and fitting the response data to a variable slope sigmoidal curve-fit function using Prism 5.0d (GraphPad, San Diego, CA). IC_{50} values represent means and standard error from at least three independent assays.

Fluorescence microscopy and image analysis

For live cell imaging, culture samples were washed twice with PBS and mounted under coverslips with Slowfade Antifade Reagent (Invitrogen) in PBS. Samples were viewed with 100X oil-immersion on either an Olympus BX61 or an AX70 Olympus PROVIS U-CMAD3 epifluorescence microscope or equipped with a 100W mercury bulb using U-MWU or U-MWB filter sets. Micrographic images were recorded using the Olympus MicroSuite (TM)-B3SV or Olympus DP70 camera system, and compiled using the Olympus DP Manager software and Adobe Photoshop CS v8.0. Mixed-stage *P. falciparum* cultures were exposed to 500 nM concentrations of trioxolane **5, 7** or **8** for 10 min in RPMI at 37 °C. Parasites were viewed directly or were first released from erythrocytes using 0.2% saponin.

Competition experiments

Mid- to late trophozoite-stage cultures were exposed to 500 nM trioxolane **8** or drug-vehicle (0.01% MeOH) in pre-warmed complete media and incubated at 37 °C. After 10 min, the media was removed and replaced with fresh, pre-warmed complete media containing 500 nM of trioxolane **5.** Following a 10 min incubation period, parasites were washed, released with 0.2% saponin and processed for microscopy. The total number of NLB positive for detectable trioxolane **5** fluorescence from each pre-treatment group was tabulated from ~10

random fields of view in three independent experiments (approximately 300 total parasites per treatment group) and divided by the total number of parasites counted. Results were reported as the average percent decrease in fluorescently-labeled NLB among the trioxolane **8** pre-treatment groups compared to the MeOH pre-treatment control group. Statistical significance of pre-treatment effects on the average accumulation of trioxolane **5** signal between the two pre-treatment groups was evaluated using the student's t test ($p < 0.05$).

Lipid peroxidation studies using BODIPY 581/591 C_{11}

BODIPY 581/591 C_{11} peroxidation-sensitive probe (Molecular Probes) was reconstituted to 40 μM in DMSO and stored under N_2. At each asexual stage, cultures were exposed to 250 nM trioxolane **8,** ART, dDHA[20] or vehicle control (0.01% MeOH) for 2.5 h at 37 °C. Cultures were then treated with 40 nM BODIPY 581/591 C_{11} and incubated for an additional 30 min prior to imaging. Ring and segmenter-stage parasites occurred simultaneously in culture and were not saponin-released due to difficulty in pelleting freed ring-stage parasites, whereas trophozoite-stage parasites were released from erythrocytes using 0.2% saponin prior to visualization.

Synthesis - General Methods

^{1}H NMR spectra were recorded on a Varian INOVA-400 400 MHz spectrometer. Chemical shifts are reported in δ units (ppm) relative to TMS as an internal standard. Coupling constants (*J*) are reported in hertz (Hz). Synthetic intermediates 1-(hydroxymethyl)cyclohexanol, **9,** and **10,** and were prepared according to literature methods as indicated below. All other reagents and solvents were purchased from Aldrich Chemical or Acros Organics and used as received. Column chromatography was carried out using a Biotage SP1 flash chromatography system and silica gel cartridges from Biotage. Analytical TLC plates from EM Science (Silica Gel 60 F254) were employed for TLC analyses.

Purity of final compounds

All compounds studied in parasites (**5–8**) were judged to be of 95% or higher purity based on analytical LC/MS analysis. LC/MS analyses were performed on a Waters Micromass ZQ/ Waters 2795 Separation Module/Waters 2996 Photodiode Array Detector system controlled by MassLynx 4.0 software. Separations were carried out on an XTerra® MS C_{18} 5μm 4.6×50mm column at ambient temperature using a mobile phase of water-acetonitrile containing 0.05% trifluoroacetic acid. Gradient elution was employed wherein the acetonitrile-water ratio was increased linearly from 5 to 95% acetonitrile over 2.5 minutes, then maintained at 95% acetonitrile for 1.5 min., and then decreased to 5% acetonitrile over 0.5 min, and maintained at 5% acetonitrile for 0.5 min. Compound purity was determined by integrating peak areas of the liquid chromatogram, monitored at 254 nm.

Synthesis of dispiro[adamantane-2,2′-[1,3,5]trioxolane-4′,1″-cyclohexane]-5-yl 5-(dimethylamino)naphthalene-1-sulfonate (5)

To a solution of alcohol **9**[31] (0.15 g, 0.54 mmol) and 4-(dimethylamino)pyridine (0.065 g, 0.54 mmol) in anhydrous pyridine (3 mL) at 0 °C was added dropwise a solution of dansyl chloride (0.29 g, 1.07 mmol) in dichloromethane (0.2 mL). The reaction was warmed slowly to room temperature and stirred overnight, at which time an additional five equivalents of dansyl chloride were added and the reaction left to stir for an additional 72 h. The reaction mixture was then concentrated *in vacuo* and ethyl acetate and water were added. The aqueous layer was separated and extracted with EtOAc (3 x 5 mL). The organic layers were combined and washed with water and brine, and then dried ($MgSO_4$), filtered and concentrated. The crude residue was purified by automated silica gel flash chromotagraphy (7% EtOAc/hexanes) to afford the trioxolane **5** as a mixture of stereoisomers (0.079 g, 0.15

mmol, 29%): IR 2938, 2864, 2787, 1574, 1451, 1354, 1173, 1115, 1092, 1071 cm^{-1}; ^1H NMR (400 MHz, $CDCl_3$) δ 8.56 (dd, *J* = 8.4, 3.6 Hz, 1H), 8.22–8.31 (m, 2H), 7.49–7.60 (m, 2H), 7.19 (dd, *J* = 7.6, 3.2 Hz, 1H), 2.89 (s, 6H), 2.26–2.50 (m, 2H), 2.03–2.21 (m, 7H), 1.79–1.91 (m, 2H), 1.50–1.70 (m, 10H), 1.30–1.45 (m, 2H),; ^{13}C NMR (100 MHz, $CDCl_3$) δ 151.8, 135.8, 135.7, 130.9, 130.0, 129.9, 128.7, 128.4, 128.4, 123.3, 123.3, 119.9, 119.9, 115.5, 115.4, 109.8, 109.7, 109.1, 109.0, 90.2, 89.5, 45.6, 42.2, 42.0, 39.9, 39.7, 39.0, 38.7, 34.8, 34.6, 33.0, 33.0, 30.0, 29.6, 25.0, 23.9; LRMS calculated for $C_{28}H_{35}NO_6$ 513.65, found ($M+H^+$) 514.7.

Synthesis of 5-(dimethylamino-N-[3-({dispiro[adamantane-2,2′-[1,3,5]trioxolane-4′,1″-cyclohexane]-4″-yl}amino)propyl]naphthalene-1-sulfonamide (6)

The amine **8** (0.30 g, 0.69 mmol) was dissolved in a 4N solution of HCl in dioxane (3.6 mL). The reaction mixture was stirred for 30 min and then concentrated *in vacuo*. A quarter of the crude product was dissolved in dichloromethane (0.5 mL) and treated with dansyl chloride (0.047 g, 0.17 mmol) and triethylamine (0.06 mL, 0.4 mmol). The reaction mixture was stirred overnight protected from light. The reaction mixture was then loaded directly onto a silica gel column and eluted with 2–5% MeOH/CH_2Cl_2 to provide the trioxolane **6** as a mixture of stereoisomers (8.1 mg, 0.014 mmol, 8% over 2 steps): ^1H NMR (400 MHz, $CDCl_3$) δ 8.49–8.55 (m, 1H), 8.20–8.33 (m, 2H), 7.47–7.59 (m, 2H), 7.15–7.21 (m, 1H), 2.97–3.04 (m, 2H), 2.89 (s, 6H), 2.57–2.64 (m, 2H), 2.35–2.45 (m, 1H), 1.48–2.02 (m, 22H), 1.25–1.34 (m, 2H); ^{13}C NMR (100 MHz, $CDCl_3$) δ 152.1, 135.0, 130.2, 130.0, 129.8, 129.7, 128.4, 123.3, 119.1, 115.3, 111.6, 108.3, 55.1, 46.1, 45.6, 43.8, 36.9, 36.5, 35.0, 34.9, 32.9, 30.0, 28.0, 27.0, 26.6; LRMS calculated for $C_{31}H_{43}N_3O_5S$ 569.29, found ($M+H^+$) 570.25.

Synthesis of dispiro[adamantane-2,2′-[1,3]dioxolane-4′,1″-cyclohexane]-5-yl 5-(dimethylamino)naphthalene-1-sulfonate (7)

To a mixture of ketone **12** (0.050 g, 0.125 mmol) and 1-(hydroxymethyl)cyclohexanol[32] (0.021 mg, 0.16 mmol) in dichloromethane (1.5 mL) was added camphor sulfonic acid (0.035 g, 0.15 mmol). The reaction mixture was stirred 48 h at room temperature and then was washed sequentially with a saturated solution of $NaHCO_3$, water, brine, and dried ($MgSO_4$), filtered, and concentrated. The crude residue was purified by automated silica gel chromatography (10% EtOAc in hexanes) to provide **7** as a mixture of stereoisomers (0.046 g, 0.09 mmol, 72%): IR 2933, 2860, 2788, 1589, 1576, 1478, 1453, 1387, 1354, 1342, 1203, 1193, 1173, 1123, 1100, 1062, 1045, 1024 cm^{-1}; ^1H NMR (400 MHz, $CDCl_3$) δ 8.53–8.56 (m, 1H), 8.23–8.33 (m, 2H), 7.50–7.60 (m, 2H), 7.17–7.20 (m, 1H), 3.67–3.68 (m, 2H), 2.89 (s, 6H), 2.41–2.48 (m, 2H), 1.82–2.14 (m, 9H), 1.32–1.66 (m, 12H); ^{13}C NMR (100 MHz, $CDCl_3$) δ 151.8, 151.7, 163.0, 130.8, 130.8, 130.1, 130.0, 129.9, 128.37, 128.7, 128.3, 128.3, 123.3, 120.1, 115.4, 109.3, 91.3, 91.0, 81.0, 80.9, 74.1, 73.6, 45.6, 42.6, 42.4, 40.8, 40.7, 40.0, 39.9, 37.0, 36.9, 33.0, 33.0, 30.2, 29.9, 25.5, 23.8, 23.7; LRMS calculated for $C_{29}H_{37}NO_5S$ 511.24, found ($M+H^+$) 512.5.

Synthesis of tert-butyl N-[3-({dispiro[adamantane-2,2′-[1,3,5]trioxolane-4′,1″-cyclohexane]-4′-yl)amino)propyl]carbamate (8)

To a solution of ketone **10**[24] (0.35 g, 1.26 mmol) and commercially available *N*-Boc-1,3-propanediamine (0.26 g, 1.5 mmol) in dichloroethane (3 mL) was added sodium triacetoxyborohydride (0.40 g, 1.89 mmol). The reaction mixture was stirred for 1 h at ambient temperature and then diluted with dichloromethane, washed with saturated aqueous $NaHCO_3$, brine, and dried (Na_2SO_4), filtered, and concentrated. The crude residue was purified by automated silica gel flash chromatography (5% MeOH/CH_2Cl_2) to provide **8** as a mixture of stereoisomers (0.55 g, 1.26 mmol, >95%): ^1H NMR (400 MHz, $CDCl_3$) δ 5.13–5.17 (m, 0.14H), 3.22–3.23 (m, 2H), 2.70–2.73 (m, 2H), 2.59 (m, 1H), 1.44–2.03 (m, 24H), 1.44 (s, 9H); ^{13}C NMR (100 MHz, $CDCl_3$) δ 156.4, 111.8, 111.5, 108.5, 108.4, 79.2, 55.2,

54.9, 44.9, 44.8, 39.1, 36.9, 36.5, 36.4, 35.0, 34.9, 32.6, 32.2, 30.0, 29.8, 29.4, 28.5, 27.0, 26.6; LRMS calculated for $C_{24}H_{40}N_2O_5$ 436.29, found ($M+H^+$) 437.25.

Synthesis of 4-oxoadamantan-1-yl 5-(dimethylamino)naphthalene-1-sulfonate (12)

To a solution of 5-hydroxy-2-adamantanone (**11**) (0.15 g, 0.90 mmol) and a catalytic amount of 4-(dimethylamino)pyridine in anhydrous pyridine (1.5 mL) at 0 °C was added dropwise a solution of dansyl chloride (0.49 g, 1.81 mmol) in dichloromethane (0.2 mL). The reaction mixture was warmed to room temperature slowly and stirred overnight, at which time an additional 2 equivalents of dansyl chloride were added and the reaction mixture stirred for another 18 hours. The reaction mixture was concentrated *in vacuo* and dichloromethane and water were added. The organic layer was separated and washed with water and brine, and then dried (Na_2SO_4), filtered and concentrated. The crude residue was purified by automated silica gel chromatography (20% EtOAc in hexanes) to provide 52 mg of the desired product 12 (0.13 mmol, 14%): IR 2936, 2863, 2788, 1725, 1575, 1455, 1397, 1350, 1337, 1234, 1203, 1172, 1153, 1060, 1031 cm^{-1}; ^1H NMR (400 MHz, $CDCl_3$) δ 8.58 (d, J = 8.8 Hz, 1H), 8.25 (d, J = 7.6 Hz, 2H), 7.51–7.60 (m, 2H), 7.20 (d, J = 7.2 Hz, 1H), 2.89 (s, 6H), 2.61 (br s, 2H), 2.36–2.41 (m, 7H), 1.87–1.98 (m, 4H),; ^{13}C NMR (100 MHz, $CDCl_3$) δ 214.2, 152.0, 135.4, 131.3, 130.0, 129.9, 128.9, 128.6, 123.3, 119.6, 115.6, 87.8, 47.4, 45.6, 42.5, 41.8, 37.8, 30.6; LRMS calculated for $C_{22}H_{25}NO_4$ 399.50, found ($M+H^+$) 400.5.

Supplementary Material

Refer to Web version on PubMed Central for supplementary material.

Acknowledgments

ARR acknowledges the support of the National Institutes of Health (AI094433) and the Bill and Melinda Gates Foundation. RAC and CLH acknowledge support from the National Institutes of Health (AI055601). We would like to thank Gary H. Posner and John D'Angelo for their gift of dDHA, and acknowledge Timothy T. Stedman and ATCC for laboratory and material support (MRA-926).

References

1. Guidelines for the Treatment of Malaria. World Health Organization; Geneva: 2006.
2. Ro DK, Paradise EM, Ouellet M, Fisher KJ, Newman KL, Ndungu JM, Ho KA, Eachus RA, Ham TS, Kirby J, Chang MC, Withers ST, Shiba Y, Sarpong R, Keasling JD. Production of the antimalarial drug precursor artemisinic acid in engineered yeast. Nature. 2006; 440:940–943. [PubMed: 16612385]
3. O'Neill PM, Posner GH. A medicinal chemistry perspective on artemisinin and related endoperoxides. J Med Chem. 2004; 47:2945–2964. [PubMed: 15163175]
4. Vennerstrom JL, Arbe-Barnes S, Brun R, Charman SA, Chiu FCK, Chollet J, Dong Y, Dorn A, Hunziker D, Matile H, McIntosh K, Padmanilayam M, Santo Tomas J, Scheurer C, Scorneaux B, Tang Y, Urwyler H, Wittlin S, Charman WN. Identification of an antimalarial synthetic trioxolane drug development candidate. Nature. 2004; 430:900–904. [PubMed: 15318224]
5. Charman SA, Arbe-Barnes S, Bathurst IC, Brun R, Campbell M, Charman WN, Chiu FC, Chollet J, Craft JC, Creek DJ, Dong Y, Matile H, Maurer M, Morizzi J, Nguyen T, Papastogiannidis P, Scheurer C, Shackleford DM, Sriraghavan K, Stingelin L, Tang Y, Urwyler H, Wang X, White KL, Wittlin S, Zhou L, Vennerstrom JL. Synthetic ozonide drug candidate OZ439 offers new hope for a single-dose cure of uncomplicated malaria. Proc Natl Acad Sci. 2011; 108:4400–4405. [PubMed: 21300861]
6. O'Neill PM, Barton VE, Ward SA. The molecular mechanism of action of artemisinin – the debate continues. Molecules. 2010; 15:1705–1721. [PubMed: 20336009]

7. Tang Y, Dong Y, Wang X, Sriraghavan K, Wood JK, Vennerstrom JL. Dispiro-1,2,4-trioxane Analogues of a Prototype Dispiro-1,2,4-trioxolane: Mechanistic comparators for artemisinin in the context of reaction pathways with iron(II). J Org Chem. 2005; 70:5103–5110. [PubMed: 15960511]
8. Kaiser M, Wittlin S, Nehrbass-Stuedli A, Dong Y, Wang X, Hemphill A, Matile H, Brun R, Vennerstrom JL. Peroxide bond-dependent antiplasmodial specificity of artemisinin and OZ277 (RBx11160). Antimicrob Agents Chemother. 2007; 51:2991–2993. [PubMed: 17562801]
9. Eckstein-Ludwig U, Webb RJ, van Goethem IDA, East JM, Lee AG, Kimura M, O'Neill PM, Bray PG, Ward SA, Krishna S. Artemisinins target the SERCA of Plasmodium falciparum. Nature. 2003; 424:957–961. [PubMed: 12931192]
10. Fugi MA, Wittlin S, Dong Y, Vennerstrom JL. Probing the antimalarial mechanism of artemisinin and OZ277 (arterolane) with nonperoxidic isosteres and nitroxyl radicals. Antimicrob Agents Chemother. 2010; 54:1042–1046. [PubMed: 20028825]
11. Uhlemann AC, Wittlin S, Matile H, Bustamante LY, Krishna S. Mechanism of antimalarial action of the synthetic trioxolane RBX11160 (OZ277). Antimicrob Agents Chemother. 2007; 51:667–672. [PubMed: 17145800]
12. Cardi D, Pozza A, Arnou B, Marchal E, Clausen JD, Andersen JP, Krishna S, Moller JV, le Maire M, Jaxel C. Purified E255L mutant SERCA1a and purified PfATP6 are sensitive to SERCA-type inhibitors but insensitive to artemisinins. J Biol Chem. 2010; 285:26406–26416. [PubMed: 20530490]
13. del Pilar Crespo M, Avery TD, Hanssen E, Fox E, Robinson TV, Valente P, Taylor DK, Tilley L. Artemisinin and a series of novel endoperoxide antimalarials exert early effects on digestive vacuole morphology. Antimicrob Agents Chemother. 2008; 52:98–109. [PubMed: 17938190]
14. Selmeczi K, Robert A, Claparols C, Meunier B. Alkylation of human hemoglobin A0 by the antimalarial drug artemisinin. FEBS Lett. 2004; 556:245–248. [PubMed: 14706857]
15. Robert A, Benoit-Vical F, Claparols C, Meunier B. The antimalarial drug artemisinin alkylates heme in infected mice. Proc Nat Acad Sci. 2005; 102:13676–13680. [PubMed: 16155128]
16. Creek DJ, Charman WN, Chiu FC, Prankerd RJ, Dong Y, Vennerstrom JL, Charman SA. Relationship between antimalarial activity and heme alkylation for spiro- and dispiro-1,2,4-trioxolane antimalarials. Antimicrob Agents Chemother. 2008; 52:1291–1296. [PubMed: 18268087]
17. Haynes RK, Chan WC, Lung CM, Uhlemann AC, Eckstein U, Taramelli D, Parapini S, Monti D, Krishna S. The Fe2+-mediated decomposition, PfATP6 binding, and antimalarial activities of artemisone and other artemisinins: the unlikelihood of C-centered radicals as bioactive intermediates. ChemMedChem. 2007; 2:1480–1497. [PubMed: 17768732]
18. Klonis N, Crespo-Ortiz MP, Bottova I, Abu-Bakar N, Kenny S, Rosenthal PJ, Tilley L. Artemisinin activity against Plasmodium falciparum requires hemoglobin uptake and digestion. Proc Natl Acad Sci. 2011; 108:11405–11410. [PubMed: 21709259]
19. Kannan R, Sahal D, Chauhan VS. Heme-artemisinin adducts are crucial mediators of the ability of artemisinin to inhibit heme polymerization. Chem Biol. 2002; 9:321–332. [PubMed: 11927257]
20. Hartwig CL, Rosenthal AS, D'Angelo J, Griffin CE, Posner GH, Cooper RA. Accumulation of artemisinin trioxane derivatives within neutral lipids of Plasmodium falciparum malaria parasites is endoperoxide-dependent. Biochem Pharmacol. 2009; 77:322–336. [PubMed: 19022224]
21. Hoang AN, Sandlin RD, Omar A, Egan TJ, Wright DW. The neutral lipid composition present in the digestive vacuole of Plasmodium falciparum concentrates heme and mediates beta-hematin formation with an unusually low activation energy. Biochemistry. 2010; 49:10107–10116. [PubMed: 20979358]
22. Bousejra-El Garah F, Wong MHL, Amewu RK, Muangnoicharoen S, Maggs JL, Stigliani JL, Park BK, Chadwick J, Ward SA, O'Neill PM. Comparison of the reactivity of antimalarial 1,2,4,5-tetraoxanes with 1,2,4-trioxolanes in the presence of ferrous iron salts, heme, and ferrous iron salts/phosphatidylcholine. J Med Chem. 2011; 54:6443–6455. [PubMed: 21888440]
23. Stocks PA, Bray PG, Barton VE, Al-Helal M, Jones M, Araujo NC, Gibbons P, Ward SA, Hughes RH, Biagini GA, Davies J, Amewu R, Mercer AE, Ellis G, O'Neill PM. Evidence for a common non-heme chelatable-iron-dependent activation mechanism for semisynthetic and synthetic endoperoxide antimalarial drugs. Angew Chem Int Ed. 2007; 46:6278–6283.

24. Tang Y, Dong Y, Karle JM, DiTusa CA, Vennerstrom JL. Synthesis of tetrasubstituted ozonides by the griesbaum coozonolysis reaction: diastereoselectivity and functional group transformations by post-ozonolysis reactions. J Org Chem. 2004; 69:6470–6473. [PubMed: 15357611]
25. O'Neill PM, Rawe SL, Borstnik K, Miller A, Ward SA, Bray PG, Davies J, Oh CH, Posner GH. Enantiomeric 1,2,4-trioxanes display equivalent in vitro antimalarial activity versus Plasmodium falciparum malaria parasites: Implications for the molecular mechanism of action of the artemisinins. ChemBioChem. 2005; 6:2048–2054. [PubMed: 16222725]
26. Smilkstein M, Sriwilaijaroen N, Kelly JX, Wilairat P, Riscoe M. Simple and inexpensive fluorescence-based technique for high-throughput antimalarial drug screening. Antimicrob Agents Chemother. 2004; 48:1803–1806. [PubMed: 15105138]
27. Bennett TN, Paguio M, Gligorijevic B, Seudieu C, Kosar AD, Davidson E, Roepe PD. Novel, rapid, and inexpensive cell-based quantification of antimalarial drug efficacy. Antimicrob Agents Chemother. 2004; 48:1807–1810. [PubMed: 15105139]
28. Jackson KE, Klonis N, Ferguson DJ, Adisa A, Dogovski C, Tilley L. Food vacuole-associated lipid bodies and heterogeneous lipid environments in the malaria parasite, *Plasmodium falciparum*. Mol Microbiol. 2004; 54:109–122. [PubMed: 15458409]
29. Pisciotta JM, Coppens I, Tripathi AK, Scholl PF, Shuman J, Bajad S, Shulaev V, Sullivan DJ Jr. The role of neutral lipid nanospheres in *Plasmodium falciparum* haem crystallization. Biochem J. 2007; 402:197–204. [PubMed: 17044814]
30. Drummen GP, van Liebergen LC, Op den Kamp JA, Post JA. C_{11}-BODIPY(581/591), an oxidation-sensitive fluorescent lipid peroxidation probe: (micro)spectroscopic characterization and validation of methodology. Free Radic Biol Med. 2002; 33:473–490. [PubMed: 12160930]
31. Vennerstrom, JL.; Dong, Y.; Charman, SA.; Wittlin, S.; Chollet, J.; Wang, X.; Sriraghavan, K.; Zhou, L.; Matile, H.; Charman William, N. Spiro and Dispiro 1,2,4–Trioxolane Antimalarials. WO/2009/091433. 2009.
32. Fringuelli F, Germani R, Pizzo F, Savelli G. One-Pot Two-Steps Synthesis of 1,2-Diol. Synthetic Commun. 1989; 19:1939–1943.

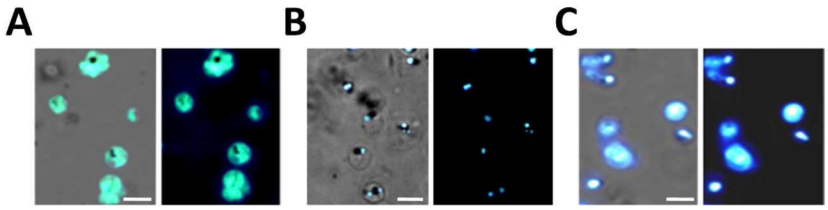

Figure 1.

Accumulation of adamantyl-tagged trioxolane derivatives within NLB of mature *P. falciparum* parasites is endoperoxide-dependent. Parasites were incubated with 500 nM of A) trioxolane **6;** B) trioxolane **5,** or; C) inactive trioxolane **7.** Fluorescence from trioxolane 6, containing the cyclohexane dansyl fluorophore, distributes within the parasite cytoplasm uniformly (A) while the adamantyl-tagged trioxolane **5** signal is seen only within spherical NLB (B). In contrast to trioxolane **5,** the inactive trioxolane derivative **7** distributes indiscriminately in the parasite, suggesting specific NLB localization requires endoperoxide activation. Images show merged fluorescence with phase contrast view (left) and fluorescence view only (right). *Scale bars represent 5 μm.*

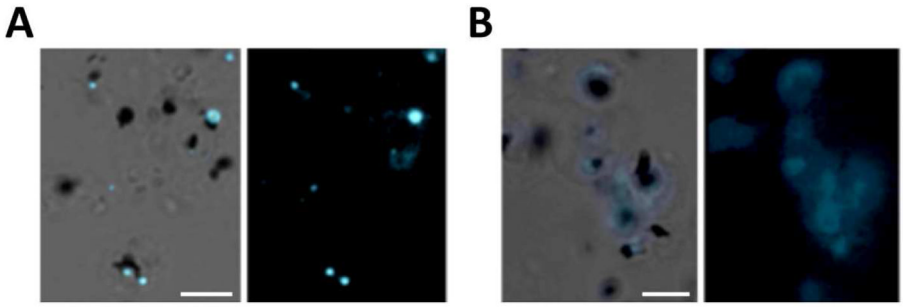

Figure 2.

Pre-incubation with unlabeled trioxolane **8** decreases trioxolane **5** accumulation within NLB of late-stage parasites. Cultures were exposed for 10 min to either A) 0.01% MeOH (drug vehicle) or B) 500 nM trioxolane **8,** followed by a 10 min exposure to 500 nM trioxolane **5.** A) Cultures pre-incubated with MeOH show intense labeling of NLB upon exposure to trioxolane **5** compared to (B) parasites pre-incubated with trioxolane **8,** demonstrating competion between the two compounds. Images show phase contrast merged with fluorescence view (left) and fluorescence view only (right). *Scale bars represent 5 μm.*

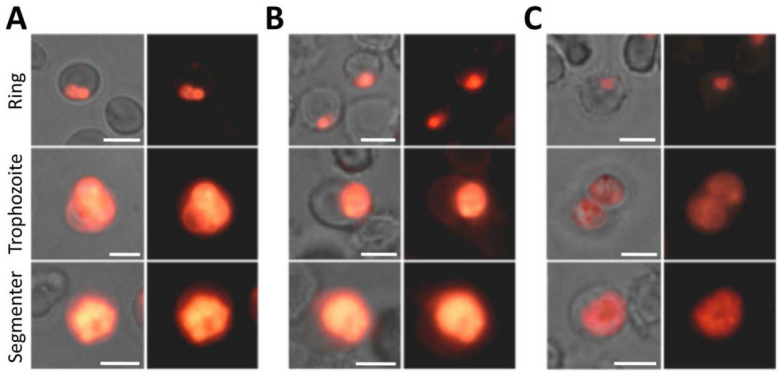

Figure 3.

Trioxolane exposure induces peroxidation of parasite membrane-incorporated BODIPY 581/591 C_{11} radical sensor probe, similar to the trioxane ART. Cultures were treated for 2.5 h with 250 nM A) trioxolane **8,** B) ART or C) the non-peroxidic artemisinin analog dDHA, prior to a 0.5 h exposure to BODIPY probe. Rows represent asexual parasite stages. Trioxolane exposure induces probe peroxidation (indicated by the yellow emission shift) in all asexual stages, similar to the ART control group, while the inactive derivative fails to induce probe peroxidation. Left columns show merged fluorescence with phase contrast view, while right columns show fluorescence only. *Scale bars represent 5 μm*.

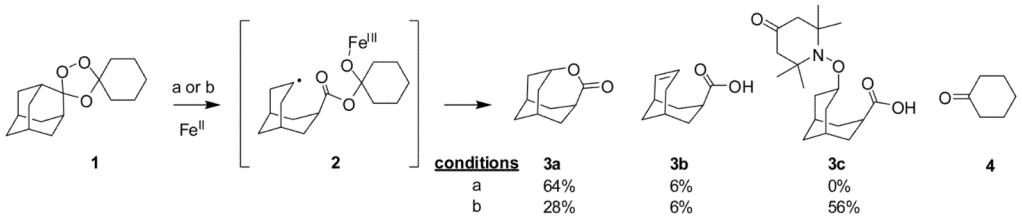

Scheme 1.

Likely mechanism and observed products[7,10] in the reaction of 1,2,4-trioxolane **1** with inorganic ferrous iron. Reaction conditions: a) 1.0 equivalent ferrous bromide, tetrahydrofuran; b) 1.5 equivalents ferrous acetate, water-acetonitrile (1:1), 2.0 equivalents 4-(oxo)-TEMPO.

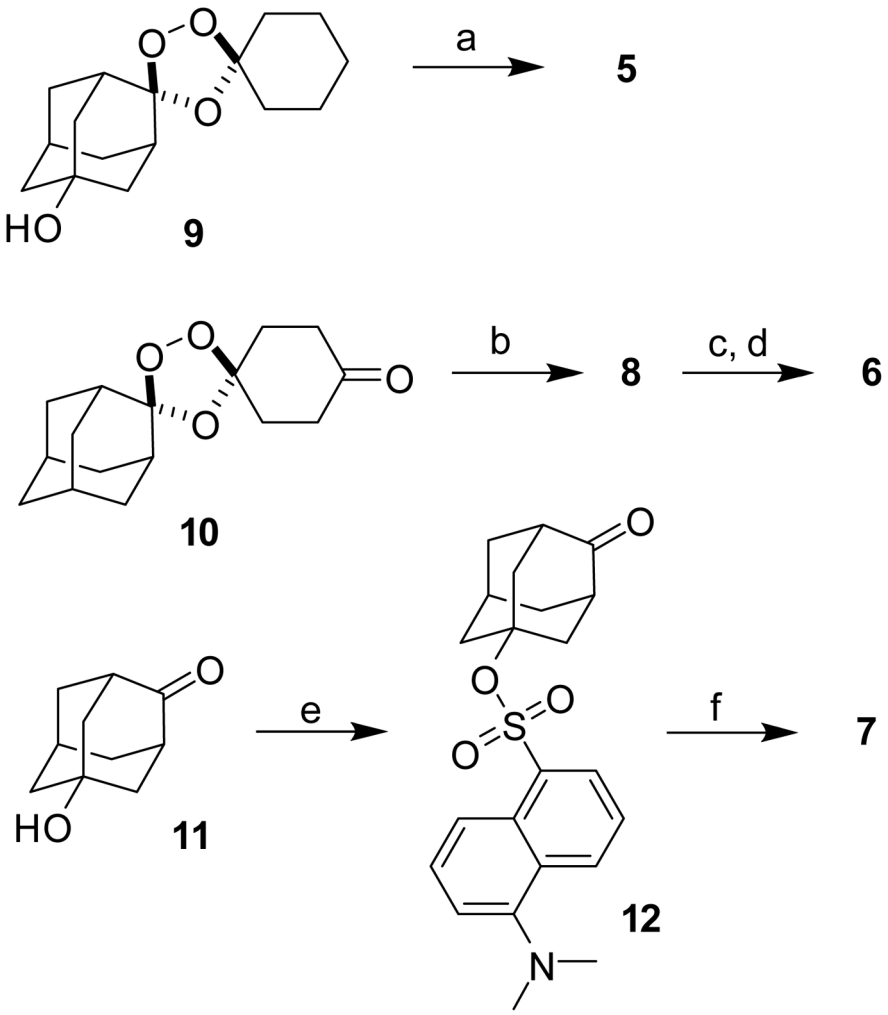

Scheme 2.

Synthesis of chemical probes **5–8**. Conditions: a) dansyl chloride, DMAP, pyridine, 29%; b) *N*-Boc-1,3-propanediamine, $NaBH(OAc)_3$, dichloroethane, 95%; c) 4N HCl, dioxane; d) dansyl chloride, triethylamine, dichloromethane, 8% over two steps; e) dansyl chloride, DMAP, pyridine, 14%; f) 1-(hydroxymethyl)cyclohexanol, camphor sulfonic acid, dichloromethane, 72%.

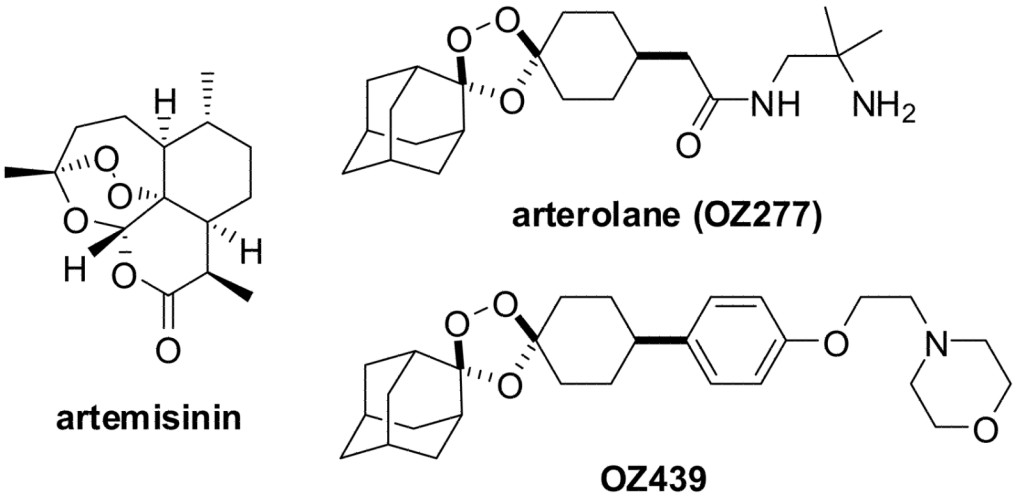

Chart 1.

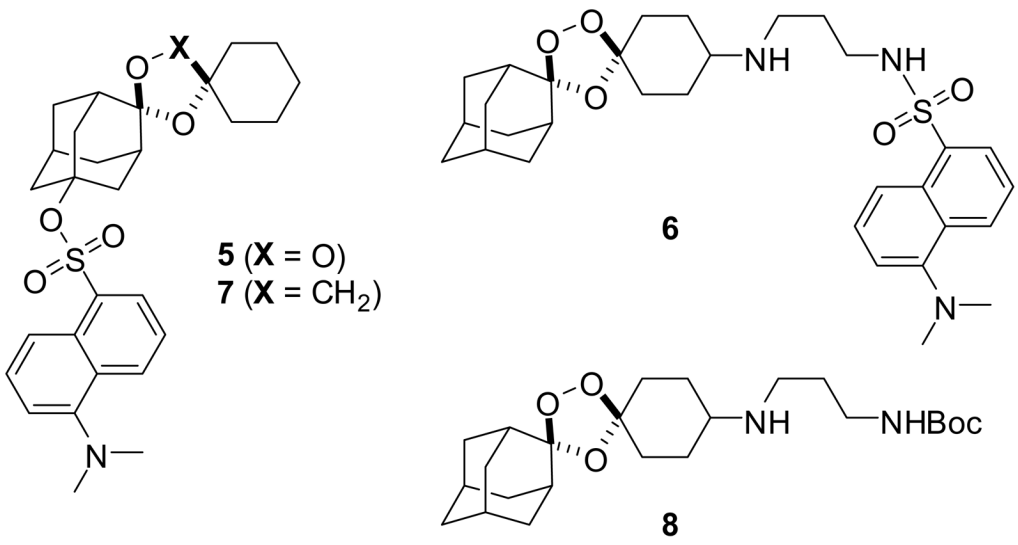

Chart 2.

Table 1

Growth inhibitory activities of artemisinin, arterolane, and compounds **5–8** against intraerythrocytic ring stage *P. falciparum* parasites.

Compound	IC_{50} ± SEM (nM)	*P. falciparum* strain
artemisinin	8.0 ± 0.1	FCB
arterolane	2.5 ± 0.3 [a]	K1
5	17.9 ± 0.9	FCB
6	14.6 ± 1.1	FCB
7	24990 ± 1363	FCB
8	12.6 ± 0.4	FCB

[a] IC_{50} value from reference 4.